

Implementation and Study of Grid-Connected Control for Distributed Generation System

JIANFEI ZHAO, XINGWU YANG, JIANGUO JIANG

Department of Electrical Engineering

Shanghai Jiao Tong University

Shanghai 200240

P.R.CHINA

zifei@sjtu.edu.cn

Abstract: - An intelligent grid-connected control system for distributed generation system is proposed and studied. The proposed control system consists of reactive power compensation control strategy, dead-time compensation control strategy, voltage and current control strategy, anti-islanding control strategy, and so on. The interrelationships of the control strategies are also developed so as to form an intelligent and integrated protection system for the distributed generation system. A 10 kW power conditioner which consists of a dc-dc boost converter and a three-phase dc-ac voltage source inverter is established. Experimental results show that the power conditioner with the proposed control system can operate with high efficiency, high power factor and low current and voltage total harmonic distortion in a wide output range. Thus, it can be considered as a total solution of the control strategy for distributed generation system.

Key-Words: - Grid-Connected Control, Distributed Generation System, Anti-Islanding Detection, Total Harmonic Distortion, DC-DC Boost Converter, DC-AC Voltage Source Inverter

1 Introduction

Nowadays, with the environmental problem caused by the use of traditional energy and the acute conflict between the limited natural resources and the demand for energy, the necessity of producing more energy combined with the interest in clean technologies yields in an increased development of power distribution systems using renewable energy [1,2]. Among the renewable energy sources, wind energy source and photovoltaic energy source have been widely utilized. So, many control strategies have been developed for three-phase voltage source inverter (VSI) in distributed generation system [2-5]. In these researches, the space vector modulation (SVM) and the current control for three-phase inverter are mainly focused on. Some special control strategies which may be suitable for distributed generation system are developed in recent years [6-11]. The control strategy researches are all mainly focused on one or more parts of the whole control system. There is also an overview of them described in [1].

In this paper, an intelligent control system for the grid-connected distributed generation system is proposed. The control system consists of ac voltage rise restraint control, dc link voltage rise restraint control, dc link constant voltage control, dead-time compensation control, capacitor charge control, recover capacitor compensation control, passive

anti-islanding detection and active anti-islanding detection, and so on. The interrelationships of these control parts are also analyzed in detail because there are many interrelationships in different control parts and protections of the system. A design example of a 400V of 10 kW design example, featured by high efficiency, high power factor and low total harmonic distortion (THD), is developed, and also confirmed by experimental results.

This paper is organized as follows: the hardware topology is described in Section 2. Control system and control strategy are discussed in Section 3. A design example and experimental results are presented in Section 4. Finally, the conclusions are given in Section 5.

2 Structure of hardware topology

A three-phase grid-connected distributed generation system is shown in Fig. 1, which has a typical dc-dc-ac topology with a dc link boost chopper and a three-phase inverter. In this topology, a basic boost chopper maintains the dc link voltage at an appropriate level to ensure a high quality current feeding into the grid even at a low dc input voltage, and a typical three-phase intelligent power module full-bridge PWM VSI is connected to the grid through an inductor and capacitor filter and an electromagnetic relay. The control platform of the entire system is built on a digital signal processor.

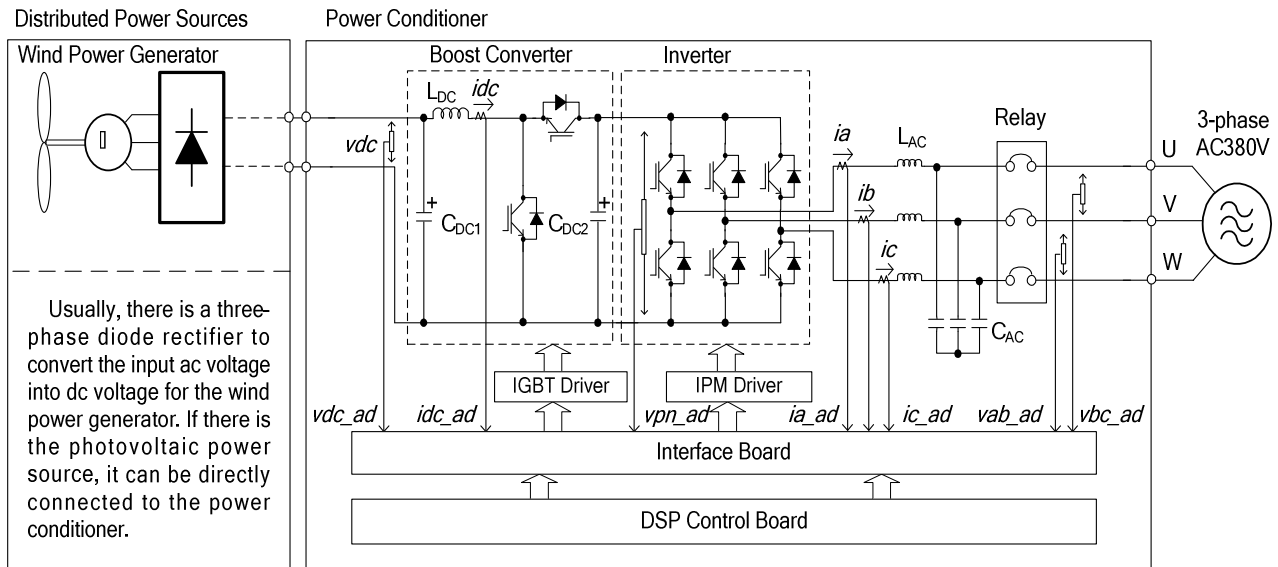


Fig.1 Block diagram of grid-connected power conditioner for distributed generation system

3 Structure of Control System

The proposed control system of grid-connected distributed generation system is described in Fig. 2. For the inverter, the voltage space vector pulse width modulation (SVPWM) is used to generate PWM patterns of IPM driver. The d-axis reference current i_{d_ref} is the output of the dc link constant voltage control. The q-axis reference current i_{q_ref} is the sum of the outputs of active anti-islanding control, recover capacitor compensation control and ac voltage rise restraint control. To reduce the current THD, dead-time compensation control is

also necessary. For the boost converter, capacitor charge control, maximum power point tracking (MPPT) control and dc link voltage rise restraint control are applied to generate the dc reference current i_{dc_ref} used in the dc current control. These control strategies are combined by interrelationships to form a total solution of the control system that also has the protection functions.

The details of the control system will be described in the following from sections 3.1 to 3.9 according to the same numbers described in the Fig.2.

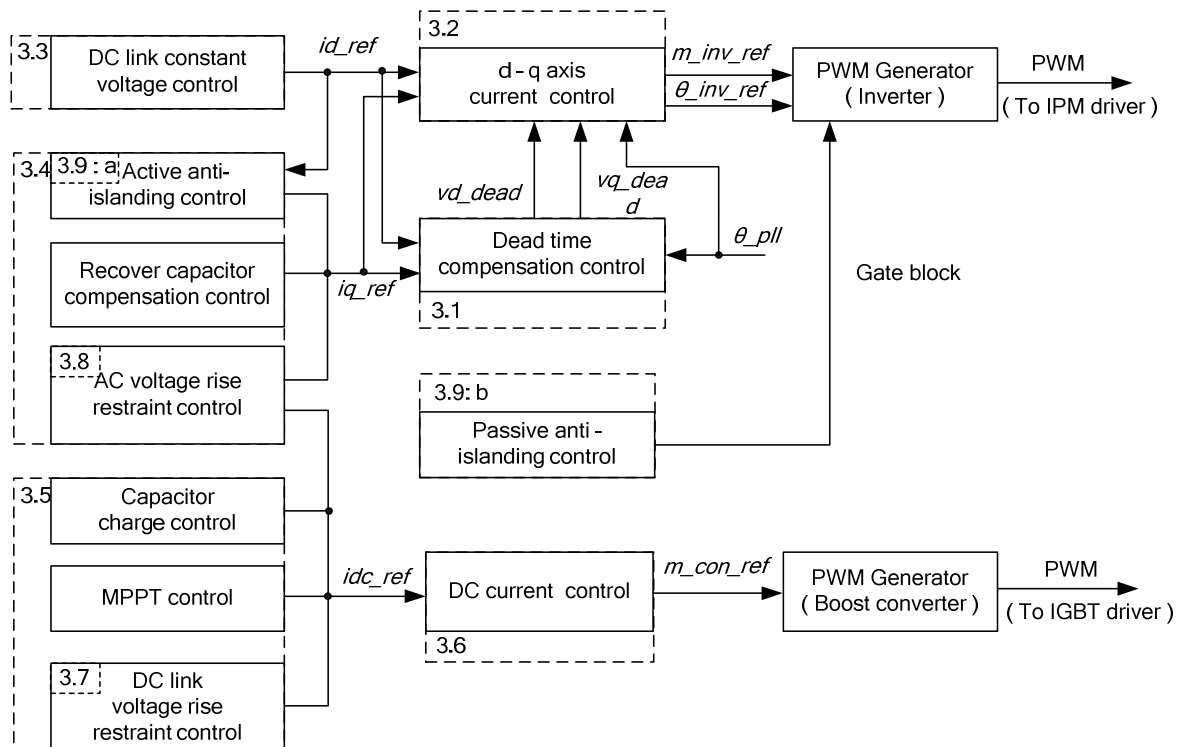


Fig.2 Block diagram of control system

3.1 Control strategy of dead-time compensation for inverter

To reduce the current THD caused by the dead-time of switches in the IPM, dead-time compensation control is demanded. The control diagram is shown in Fig. 3. The d- and q-axis reference currents can be obtained in the following section 3.3 and 3.4,. The phase θ_{pll} of voltage vector for the Clarke and inverse Clarke transform is obtained from phase lock loop (PLL). The three-

phase reference currents i_{u_ref} , i_{v_ref} or i_{w_ref} which have the same phase with voltage for PLL are the sinusoidal curves shown as (a). The compensated current curve is illustrated as solid line in (b). The gain k_{dead} of the limit is given by

$$k_{dead} = T_{dt} / T_{car}, \quad (1)$$

where T_{dt} is the period of dead-time, and the T_{car} is the period of carrier.

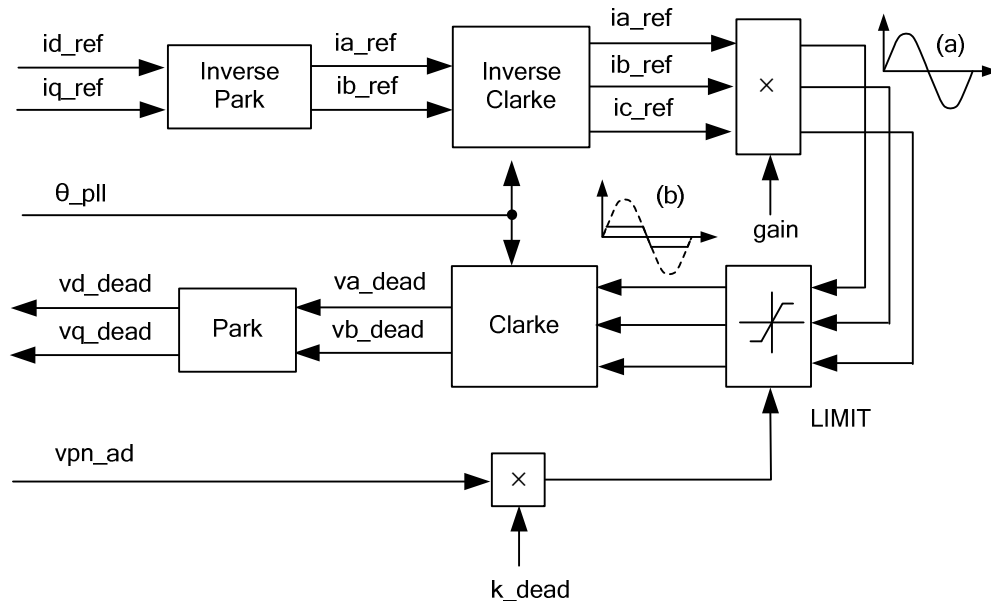


Fig.3 Block diagram of dead-time compensation control for inverter

3.2 Control strategy of d-q axis current for inverter

To generate the duty-cycle m_{inv_ref} and the phase θ_{inv_ref} for the SVPWM, the d-q axis current control is presented as Fig. 4. The a-q axis voltage outputs vd_dead and vq_dead of the dead-

time compensation control and the a-q axis voltage outputs of d-q axis current control are simultaneous used to the PWM generator of the inverter. As shown in Fig. 4, the feed forward value of the vd_ad and vq_ad are also used.

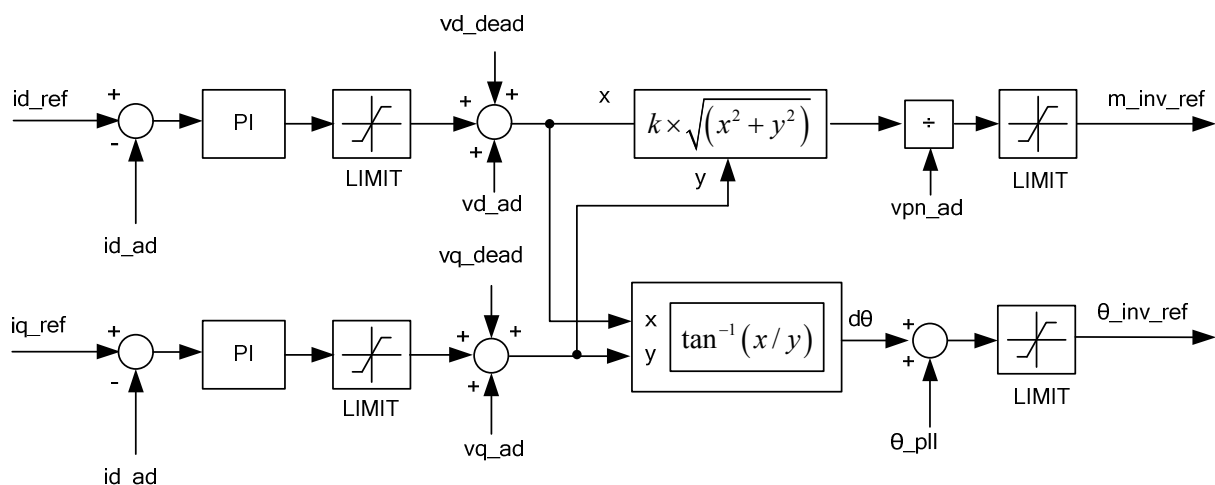


Fig.4 Block diagram of d-q axis current control for inverter

3.3 Control strategy of d-axis reference current for inverter

According to the structure of the power conditioner shown in Fig. 1, the dc link constant voltage control is necessary to obtain an appropriate constant voltage to ensure a high quality current feeding into the grid. Because the boost converter is used for the MPPT control for the distributed power sources, such as photovoltaic (PV) and wind generator (WG), the dc link constant voltage control is realized by the control of the inverter side. The

block diagram is shown in Fig. 5. The output is the d-axis reference current because the active power current of the inverter is originated from d-axis current. A soft start gain k_{soft_inv} and the original voltage of the dc link voltage vpn_start are used to reduce the impact dc link voltage vpn_ad from the control. k_{soft_start} begins at zero and ends at one. vpn_start is originated from the input voltage of distributed power source though the diode in IGBT before the relay in the ac side is switched on.

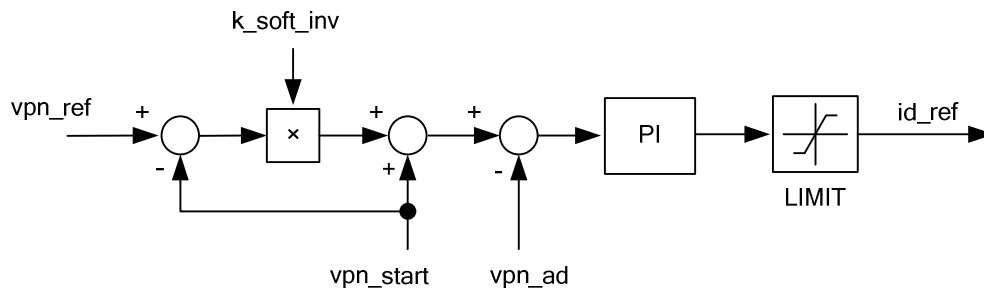


Fig.5 Block diagram of dc link constant voltage control

3.4 Control strategy of q-axis reference current for inverter

The q-axis current is the reactive current for the inverter. The control strategy is shown in Fig. 6. The reactive current iq_act_ref of anti-islanding control is one part of the q-axis reference current. It will be described in part I of this section. The reactive current iq_v_ref of the ac voltage rise restraint control is the other part of the q-axis reference current because to inject reactive power current can increase the voltage drop of the grid for increasing the inductive reactance. So, when the ac voltage of the grid is over the limit of the control system, this control method can reduce the ac voltage to inhibit the ac voltage over the limit value to some extent.

The value of active power, reactive power and the power factor is presented in section 3.8. The iq_c_ref is the reactive current for the recover capacitor compensation in the capacitor filter of the ac-side. It is given by

$$iq_c_ref = \frac{v_{sys_rms}}{X_C}, \quad (2)$$

where v_{sys_rms} is the grid voltage root mean square (RMS) value, and X_C is the capacitive reactance of recover capacitor. It is given by

$$X_C = \frac{1}{2 \times \pi \times C_{AC}}. \quad (3)$$

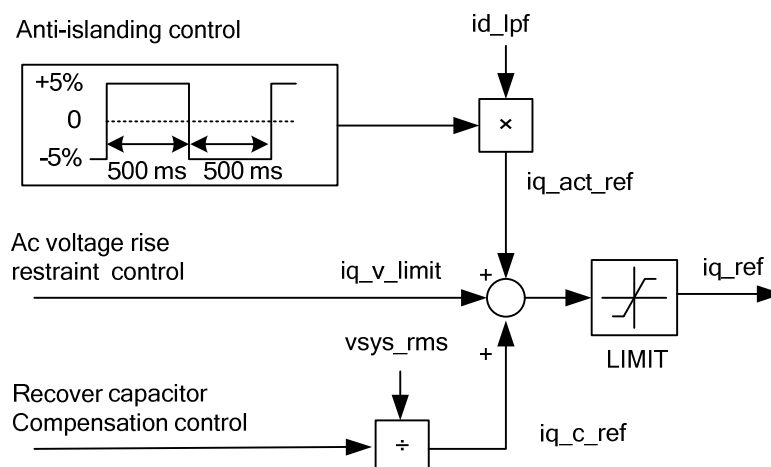


Fig.6 Block diagram of q axis reactive power current input

3.5 Control strategy of reference current for converter

The reference current input ipn_ref of the boost converter is shown in Fig. 7. As described in section 3.1, dc link constant voltage control is executed by the inverter. Before the relay in the side of ac power grid is switched on, sometimes the voltage of the dc link capacitor is very low for the low input voltage of the distributed generation source. If the relay is closed at that time, the surge current from the ac-side is so large that IPM may be destroyed. Usually, the power conditioner uses a charge resistor and another relay to deal with this problem. Thus, the size of resistor is very big for the large power loss, and the cost of another relay is necessary. For this proposed control system, before relay is closed and the dc link constant voltage control is executed, the

capacitor charge control is applied to the boost converter side. A constant charge reference current such as 1 A is used to deal with this problem. When the dc link voltage arrives at a safe level, the relay is closed and dc link constant voltage control is started. Then, the control of the boost converter is automatically switched to the MPPT control.

When the ac voltage of grid system is higher than the limit value, instead of using the reactive power current injected to the ac grid described in section 3.2, another method to reduce the ac voltage is to limit the output reference current of the MPPT by $gain_p_limit$. This will be described in section 3.8.

If the dc link voltage is higher than the limit value, another limit id_vdc_limit is applied to reduce the reference current ipn_ref .

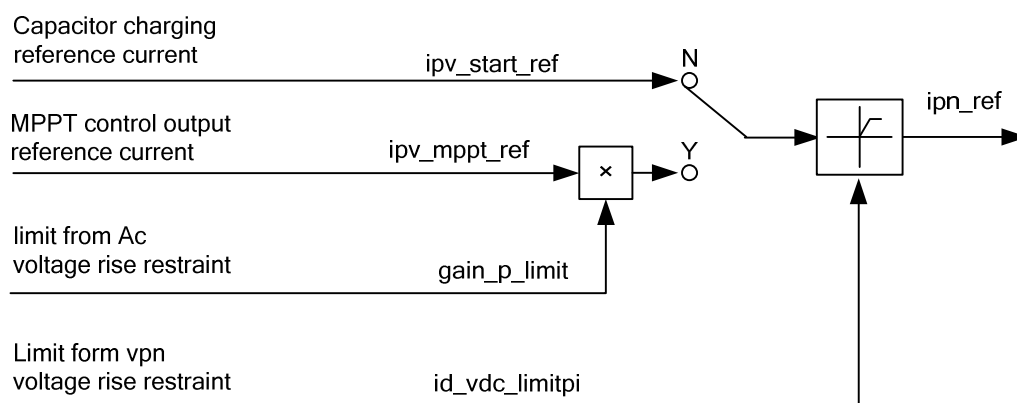


Fig.7 Block diagram of reference current for converter

3.6 Control strategy of current control for converter

The current ipn_ref described in section 3.5 is

applied for the current control to generate PWM for the boost converter. The diagram is shown in Fig. 8.

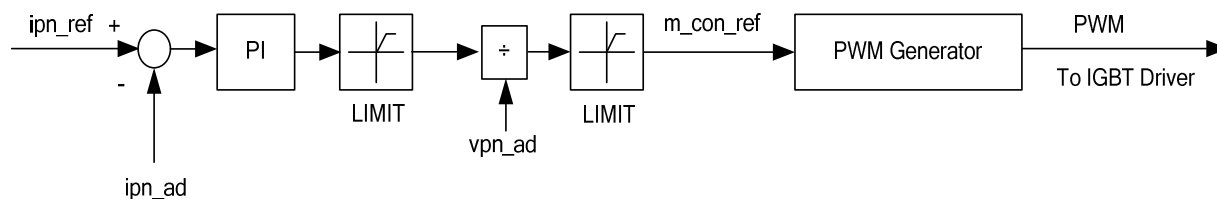


Fig.8 Block diagram of current control for converter

3.7 Control strategy of dc link voltage rise restraint for converter

As described in section 3.5, when the dc link voltage is higher than the limit value vpn_limit_ref , the dc link voltage rise restraint control shown in Fig. 9 is executed to reduce the output current of the

converter because the inverter can not delivery much more power to the ac power grid system. Here, another soft start gain k_soft_con for the converter is also used to reduce the impact of the inhibition control.

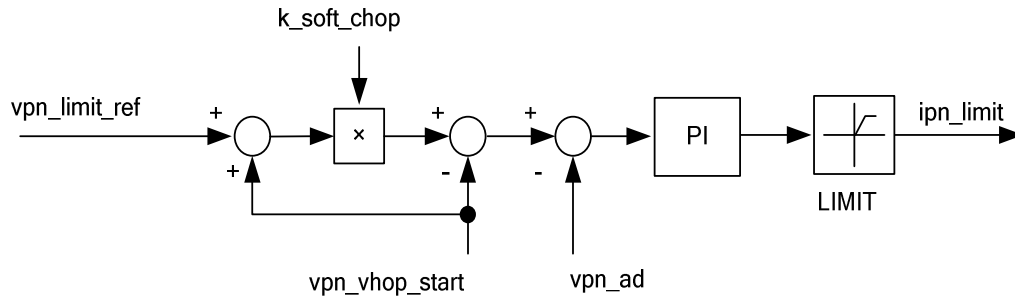


Fig.9 Block diagram of dc link voltage rise restraint control

3.8 Control strategy of ac voltage rise restraint for inverter and converter

In section 3.2 and 3.5, a control strategy called ac voltage rise restraint control is mentioned. It is executed when the maximum ac voltage v_{sys_max} is up to the limit value v_{sys_limit} . One reason may be that the voltage quality in some factory is bad for the operations of equipments sometimes. The other reason may be that the impedance of the ac power grid is so large that the voltage is increasing when power conditioner regenerates power to the grid. Thus, the ac voltage rise restraint control is necessary, and the block diagram is described in Fig. 10. The $i_{q_pf_limit}$ coming from the limit of the power factor (PF) is given by

$$i_{q_pf_limit} = i_{d_lpf} \times \tan(36.87^\circ), \quad (4)$$

where i_{d_lpf} is the d-axis current of the inverter.

$$\tan(36.87^\circ) = 0.8, \quad (5)$$

When the v_{sys_max} is higher than v_{sys_limit} , if the injected q-axis current $i_{q_v_limit}$ is higher than $i_{q_pf_limit}$, the $gain_p_limit$ is decreased to limit the boost converter output not to generate more power to the ac grid as shown in Fig. 10. It is because that the PF is lower than 0.8 at this time. When the v_{sys_max} is higher than v_{sys_limit} , if the PF is also higher than 0.8, the q-axis current $i_{q_v_limit}$ of the inverter is increased to inject reactive power into ac power grid described in Fig. 6. Thus, the inductive reactance can be increased for more voltage drop of the ac grid voltage, and the active power regenerated from power conditioner to the ac power grid is not decreased. When the ac grid voltage is dropped under the limit voltage, the reactive power current $i_{q_v_limit}$ will return to the zero. Then, the limit the output reference current $gain_p_limit$ is set to maximum value.

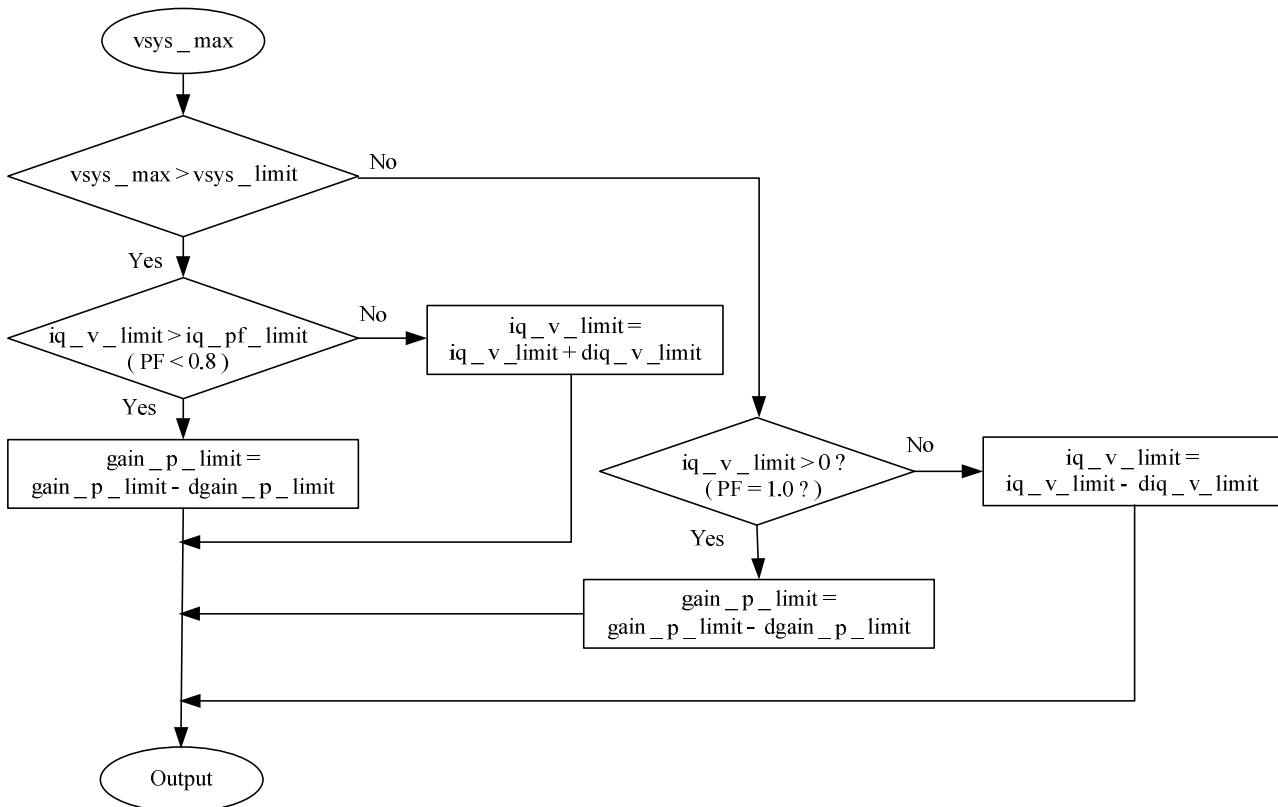


Fig.10 Block diagram of ac voltage rise restraint control

3.9 Control strategy of anti-islanding detection

Islanding detection method is applied in the distributed generation system to prevent the power conditioner regenerating the power to the ac power grid when the ac power grid is default.

a) Passive islanding detection.

Passive methods for detecting an islanding condition basically monitor parameters to stop converting power when there is sufficient transition from normal specified conditions. In this paper, a voltage phase jump detection method is presented. The voltage phase of the ac power grid is detected by PLL. When the voltage phase jumps out of the allowable range, the islanding condition will be

detected by the controller. To prevent the effect of the noise in PLL, a moving average method by 10 cycles of ac voltage is used.

b) Active islanding detection

Active methods for detecting the island introduce deliberate changes or disturbances to the connected circuit and then monitor the response to determine if the ac power grid with its stable frequency, voltage and impedance is still connected. The method used in this system is to inject reactive power described in Fig. 6. The current value $i_{q_acf_ref}$ is given by

$$i_{q_acf_ref} = i_{d_ad} \times (\pm 5\%). \quad (6)$$

The pulse frequency is 1Hz, and the pulse amplitude is 5% of the active power current.

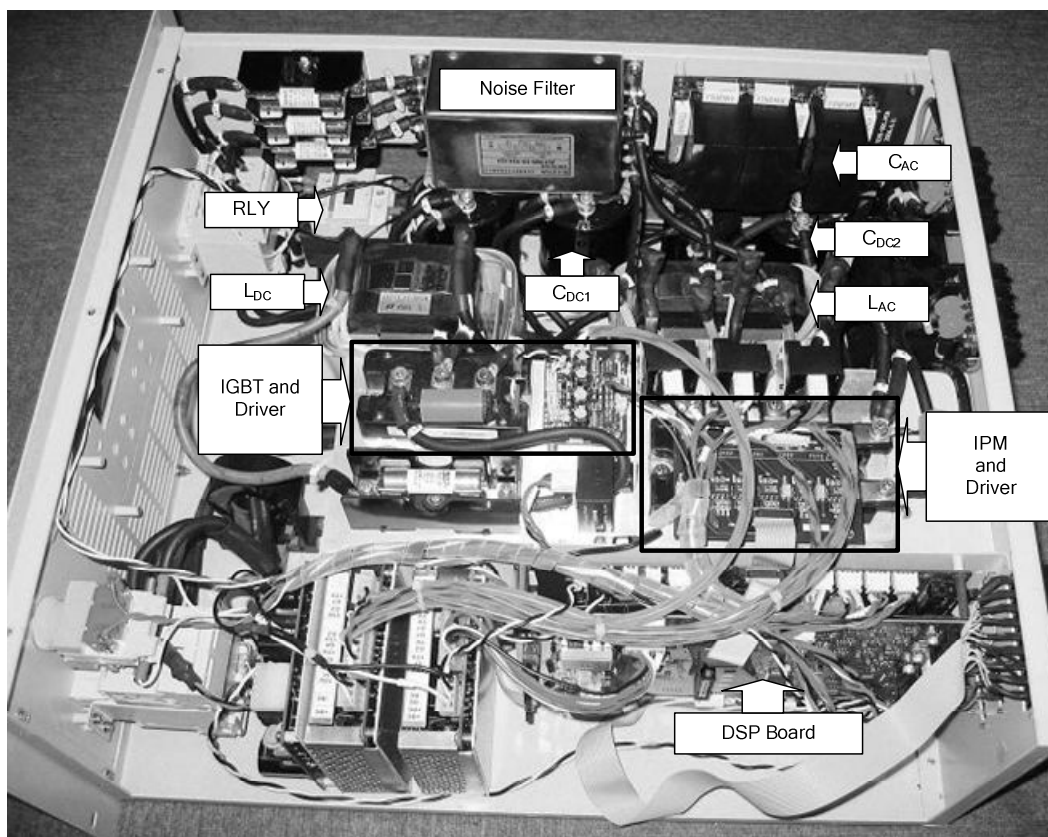


Fig.11 Pictorial view of experimental prototype

4 Design example and experimental results

Based on the circuit in Fig. 1 and the control strategy of Fig. 2, a grid-connected power conditioner for distributed generation system of 10kW is designed as shown in Fig. 11.

According to the theoretical analysis in section 2 and 3, the parameters of the main components in the power conditioner are given in Table 1.

The specifications of the power conditioner designed are shown in Table 2.

Table 1 Circuit parameters in Fig.1

Item	Symbol	Parameter
AC inductor	L_{AC}	2.7mH,15A
AC capacitor	C_{AC}	15uF,450V
DC inductor	L_{DC}	2.5mH,28A
DC input capacitor	C_{DC1}	3300uF,450V
DC bus capacitor	C_{DC2}	2200uF,400V

Table 2 Specifications of the design example

AC/DC	Item	Parameter
AC	Rated voltage	380V \pm 10%
	Power factor	>0.98
	Rated capacity	10kVA
DC	Voltage range	0 ~ 650Vdc
	Current range	0 ~ 25Adc
	Maximum power	10kW

Fig. 12 shows the specifications of the proposed power conditioner in the rating condition. The results show that the power conditioner has a power factor λ_{12} of 0.9940 and an efficiency η_1 of 92.66%. The THD of each phase current in ac-side is lower than 2.68 % and the THD of the voltage is lower than 1.09 % in the last four items shown in the Fig 12.

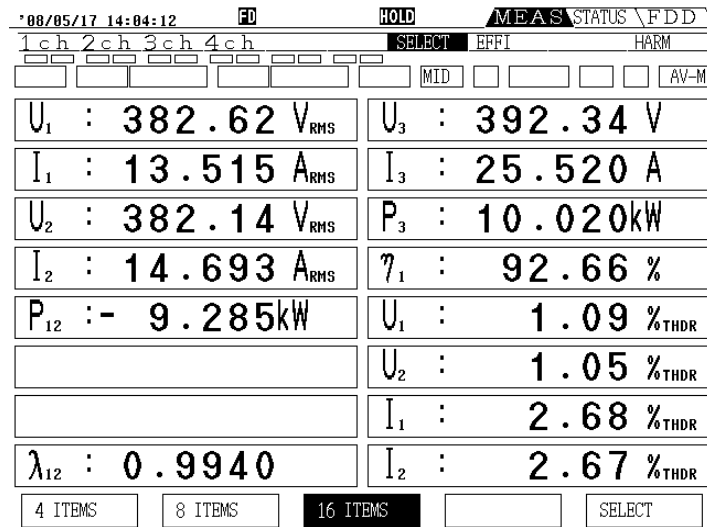


Fig.12 Experimental results of rating operation. U_1 , U_2 , I_1 and I_2 are the ac input line voltage and line current, P_{12} , Q_{12} and S_{12} are the input active power, reactive power and apparent power. λ_{12} is power factor. U_3 , I_3 and P_3 are the output voltage, current and power in the dc-side. η_1 is the efficiency of the converter. The THD of U_1 , U_2 , I_1 and I_2 are in the last four items.

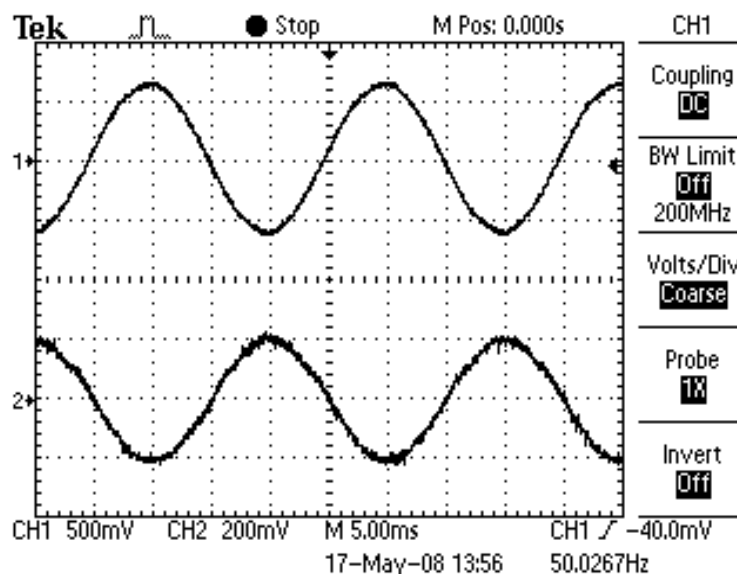


Fig.13 Experimental waveforms of grid voltage and current of rating operation. v_a (CH1):250V/div, i_a (CH2): 20A/div

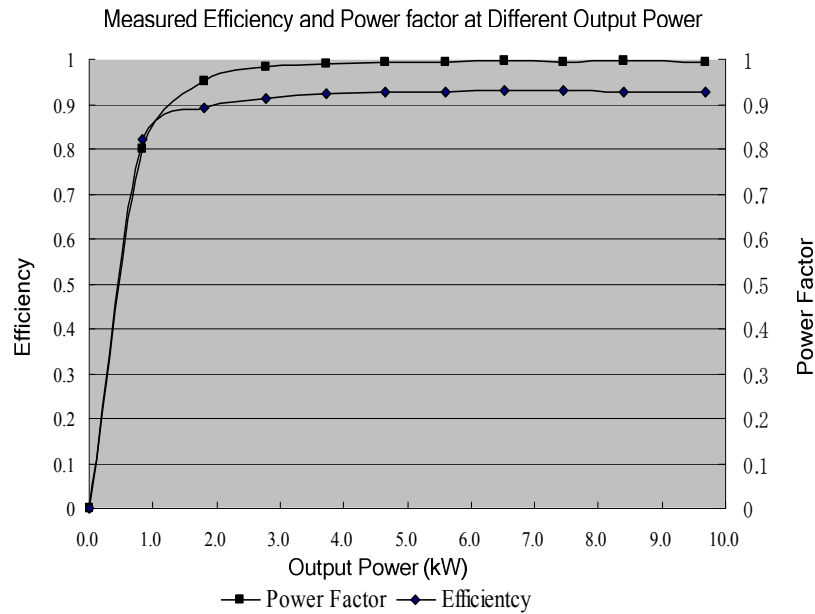


Fig.14 Efficiency and power factor curve

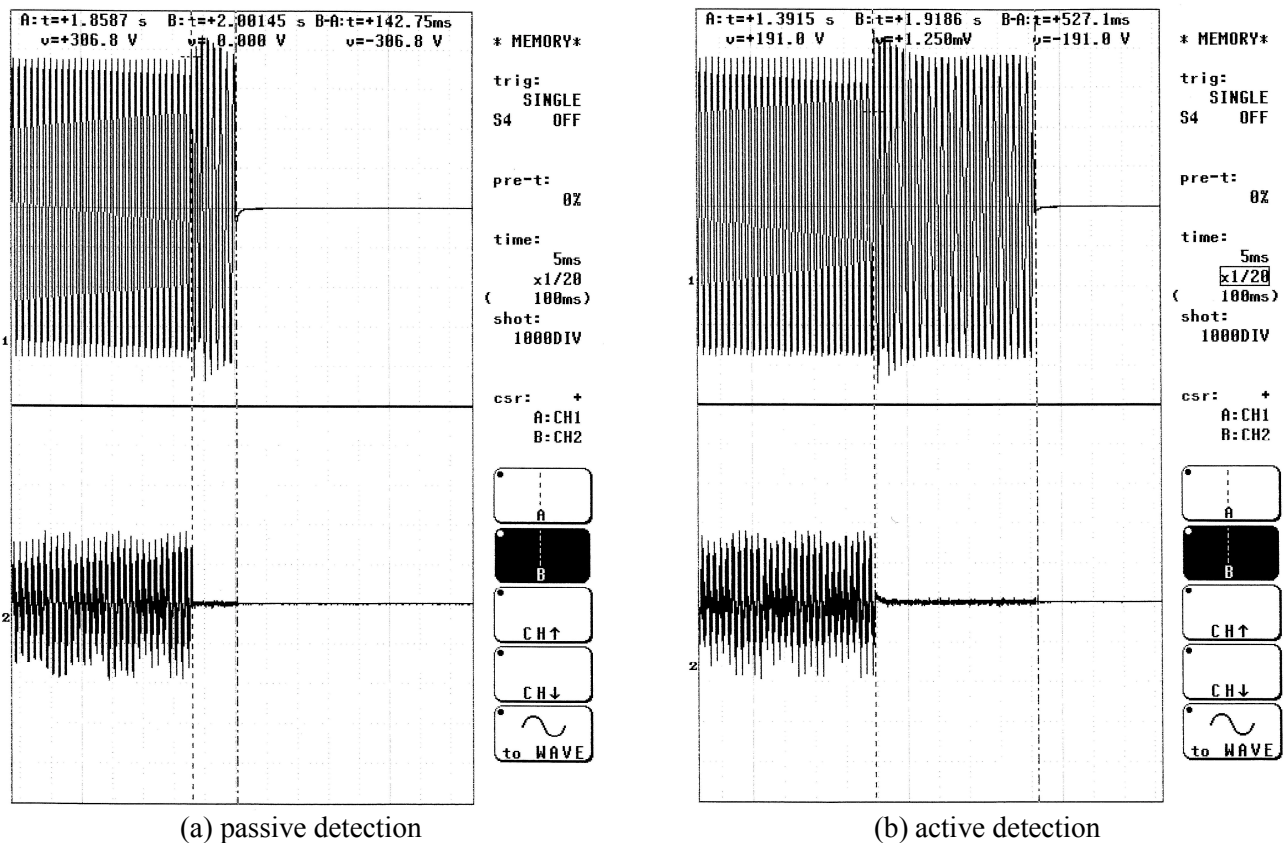
Fig.15 Experimental waveforms of anti-island capability. v_u (CH1):80V/div, i_u (CH2): 5A/div

Fig. 13 shows the experimental curves of ac grid voltage v_a and current i_a at rating condition. i_a is in phase with v_a , and they are both very near sinusoidal curve with low distortion.

Fig. 14 shows the experimental results of efficiency and power factor with different output

power from 1 kW to 10 kW. The power conditioner has a peak efficiency of 92.93% at 6.5kW, and can be operated with an efficiency of higher than 91% when the output power is above 2.5 kW. The power factor is higher than 0.98 during a wide range from 2.5kW to 10 kW. According to the analysis and experimental results, the proposed power

conditioner can work with high efficiency and high power factor in wide power output range.

Fig. 15 shows the experimental results of passive anti-landing and anti-active landing detection. The passive anti-detection is shown in Fig. 15(a). The detection period is 143 ms because the phase jump detection uses a moving average of 10 cycle period of the voltage. The active anti-detection is shown in Fig. 15(b). The detection period is 527 ms for the 1Hz reactive power injected into the ac power grid. When the active anti-islanding detection experiment is executed, the passive anti-islanding detecting is forbidden because the passive anti-islanding detection will be faster than the active anti-island by cutting off the ac power grid system.

5 Conclusion

An intelligent control system of the control system for the distributed generation system is proposed according to the hardware topology with a boost converter and a three-phase full bridge inverter. The control system considers many aspects of the grid-connected system, such as the ac voltage rise restraint, dc link voltage rise restraint, passive anti-islanding and active anti-islanding detection, and so on.

In addition, a design example rated at 400V, 10kW with proposed control system has also been developed and tested as well. The power conditioner can be operated with high power factor, high efficiency and low THD in a wide output power range. So, the design example and experiment results demonstrate the validity of the proposed power hardware structure and the control system. Therefore, It can be used in the distributed generation system such as photovoltaic power source system, wind power source system and fuel cell power source system.

Acknowledgements

This work is supported by National 973 Project (2005CB221505) and Research Fund for the Doctoral Program of Higher Education (20050248058).

References:

- [1] F. Blaabjerg, R. Teodorescu, M. Liserre, and A. V. Timbus, Overview of Control and Grid Synchronization for Distributed Power Generation Systems, *IEEE Trans. Power Syst.*, Vol. 53, No. 5, 2006, pp. 1398-1409.
- [2] M. Kimura, S. Nagai, Y. Ito, T. Sakurai, Practical Implementation of V-connection power conditioner for 10kW wind power

- generation, *Proc. IEEE PCC*, Vol. 1, 2007, pp. 1450-1455.
- [3] B. H Kwon, T. W Kim, and J. H Youm, A novel SVM-based hysteresis current controller, *IEEE Tran. Power Electron.*, Vol. 13, No. 2, 1998, pp. 297-307.
- [4] Qingrong Zeng and Liuchen Chang, Study of advanced current control strategies for three-phase grid-connected pwm inverters for distributed generation, *Proc. IEEE CCA*, 2005, pp. 1311-1316.
- [5] R. Brough, S. Crimp, A. Gardiner, H. Laird, and S. Round, Design and implementation of a direct-connected 11 kV power conditioner, *Proc. IEEE-IAS Annu. Meeting*, Vol. 2, 2003, pp. 1189-1194.
- [6] C. J. Hatziadoniu, E. N. Nikolov, and F. Pourboghrat, "Power conditioner control and protection for distributed generators and storage," *IEEE Trans. Power Syst.*, Vol. 18, No. 1, pp. 83-90, February 2003.
- [7] A. Bertani, C. Bossi, F. Fornari, S. Massucco, S. Spelta, and F. Tivegna, A microturbine generation system for grid connected and islanding operation, *Proc. IEEE PES*, Vol. 1, 2004, pp. 360-365.
- [8] A. Sakhare, A. Davari, and A. Feliachi, Fuzzy logic control of fuel cell for stand-alone and grid connection, *Journal of Power Sources*, Vol. 135, No. 1-2, 2004, pp. 165-176.
- [9] Jinhwan Jung and Kwanghee Nam, A PI-type dead-time compensation method for vector-controlled GTO inverters, *IEEE Trans. Ind. Appl.*, Vol. 34, No. 3, 1998, pp. 452-457.
- [10] A. C. Oliveira, C. B. Jacobina, and A. M. N. Lima, Improved Dead-Time Compensation for Sinusoidal PWM Inverters Operating at High Switching Frequencies, *IEEE Trans. Ind. Electron.*, Vol. 54, No. 4, 2007, pp. 2295-2304.
- [11] N. Urasaki, T. Senjyu, K. Uezato, and T. Funabashi, Adaptive dead-time compensation strategy for permanent magnet synchronous motor drive, *IEEE Trans. Energy Conver.*, Vol. 22, No. 2, 2007, pp. 271-280.